

EFFECT OF ARTIFICIAL URINE ON THE CORROSION PROPERTIES OF AZ31 ALLOY

Leoš DOSKOČIL, Pavlína ŠOMANOVÁ, Matěj BŘEZINA, Martin BUCHTÍK

Brno University of Technology, Faculty of Chemistry, Brno, Czech Republic, EU, doskocil@fch.vut.cz

https://doi.org/10.37904/metal.2025.5148

Abstract

Due to its mechanical properties and biodegradability, AZ31 magnesium alloy is being considered as a potential material for ureteral stents. This work focuses on the interaction of AZ31 alloy with artificial urine to assess its corrosion resistance. Samples of AZ31 alloy were immersed in artificial urine for different lengths of time and then their corrosion degradation was evaluated. Scanning electron microscopy (SEM) with energy dispersive spectrometer (SEM-EDS) and Fourier transform infrared spectrometry (FTIR) were used for surface characterization and identification of corrosion products. Electrochemical behaviour was determined by potentiodynamic polarization (PDP). The results showed that the degradation of AZ31 in artificial urine decreased over time. The thickness of the corrosion products reached up to 20 μ m after one week. The corrosion products were mainly composed of phosphates. AZ31 alloy appears to be a suitable candidate for the study of magnesium ureteral stents.

Keywords: AZ31 alloy, artificial urine, ureteral stent, corrosion

1. INTRODUCTION

Magnesium alloys (Mg alloys) represent materials with a unique combination of properties that make them highly attractive for a wide range of applications. Their low density, high specific strength and excellent biocompatibility open up new possibilities in various fields of engineering and medicine [1]. In the biomedical context, Mg alloys appear to be particularly promising due to their ability to biodegrade in biological environments, thus eliminating the need for a secondary surgical procedure to remove the implant. This attribute is crucial for applications where temporary support of a tissue or organ is desired, for example in orthopedics for temporary fixation elements, in cardiovascular medicine for biodegradable stents [2,3]. Despite their considerable potential, however, Mg alloys for biomedical applications face several challenges. The main disadvantage is their rapid and uncontrolled corrosion in physiological solutions, which can lead to premature loss of mechanical integrity and the release of hydrogen gas, which can be undesirable in certain tissues [1]. Therefore, considerable efforts are devoted to the development of surface treatments and optimization of alloy compositions to control the rate of degradation and improve their bioactivity [4]. One of the little-explored, but potentially very beneficial areas of application of biodegradable Mg alloys is their application as ureteral stents. Ureteral stents are temporary medical devices inserted into the ureters to ensure their patency in various pathological conditions, such as ureteral strictures [5]. Current ureteral stents are usually made of polymers or metals that require subsequent removal, which represents an additional invasive procedure and potential risks for the patient [6]. The use of biodegradable Mg alloys as ureteral stents could eliminate this disadvantage. After fulfilling its function, the stent would gradually decompose and be naturally eliminated from the body, thus avoiding the need for further surgery for the patient. Available research suggests that research in this area is currently limited. Some in vitro studies have investigated the corrosion behaviour of various Mg alloys in a simulated urinary environment and have demonstrated the potential for controlled degradation [7, 8]. Several preclinical in vivo studies in animal models have indicated the feasibility and biocompatibility of Mg stents in the ureters, but further research is needed to optimize the material, stent design, and assess long-term efficacy



and safety [9]. The aim of this work is to investigate the impact of artificial urine (AU) on the corrosion behaviour of AZ31 alloy using corrosion tests and to characterize the corrosion products.

2. EXPERIMENTAL

AZ31 magnesium alloy samples ($15 \times 15 \times 5$ mm) were used for corrosion tests. The alloy chemical composition was determined using Glow-Discharge Optical Emission Spectroscopy (GDOES): 3.60 Al, 1.34 Zn, 0.28 Mn, 0.03 Si, 0.002 Fe, 0.01 Sn (in wt%). The samples of AZ31 alloy were ground using 320 and 1200 SiC grit abrasive papers, washed in distilled water and isopropyl alcohol and then dried by hot air.

Corrosion experiments were performed in artificial urine (AU) solutions according to literature [10]. The composition is given in **Table 1**. NaN₃ was added to the original composition to exclude microbial activity. The pH was adjusted to 6.0 at 37 °C. The pH was checked and adjusted the next day.

Table 1 Composition of artificial urine solution for corrosion	on experiments
---	----------------

Substance	Concentration (g/100 ml)	
Na ₂ SO ₄	0.1700	
Uric acid	0.0250	
Sodium citrate	0.0720	
Creatinine	0.0881	
Urea	1.5000	
KCI	0.2308	
NaCl	0.1756	
CaCl ₂	0.0185	
NH ₄ CI	0.1266	
Potassium oxalate	0.0035	
MgSO ₄ .7H ₂ O	0.1082	
NaH ₂ PO ₄ .2H ₂ O	0.2912	
Na ₂ HOP ₄ .2H ₂ O	0.0831	
NaN₃	0.0100	

Immersion tests for AZ31 alloy were carried out in 200 ml AU at 37 °C for 7 days. The mass loss was calculated from the difference between the initial mass of the sample and after collection from AU, after removing all the residues from the surface through a cleaning process. The cleaning procedure involved immersing the metallic samples in a solution containing 200 g/L chromium (VI) oxide, 10 g/L silver nitrate, and 20 g/L barium nitrate until the corrosion layer was fully removed. Subsequently, the samples were briefly rinsed in water and left to air dry before weighing.

Electrochemical experiments were performed in AU solution at 37 °C. The AZ31 alloy was placed in a corrosion cell (contact area about 1 cm²) with a volume of 320 ml. The auxiliary electrode was a platinum grid and the reference electrode was a saturated calomel electrode. Potentiodynamic polarization (Biologic, VSP-300) was performed after 1 h and 48 h with a rate of 1 mV/s in the range of -0.15 mV to +0.4 mV from the stabilization of the potential.

The morphology and elemental compositions were investigated using a scanning electron microscope (Zeiss Evo LS10; SEM) equipped with an energy dispersive spectrometer (Oxford Instruments X-max 80 mm²; EDS). The samples were gold plated to increase conductivity. Calibration was performed on single crystal silicon.



Corrosion products were characterized using FTIR (Nicolet iS10) in the spectral range 4000-400 cm⁻¹ with a resolution of 4 cm⁻¹ and an average of 128 scans.

3. RESULTS AND DISCUSSION

The surface of the AZ31 alloy was completely covered with a continuous layer of corrosion products after a week of corrosion in AU (**Figure 1**). This layer was cracked, probably due to drying of the surface after the corrosion process was completed. Crystals, identified as struvite by EDS analysis, were observed only at the edges of the corroded area.

The thickness of the corrosion products was approximately 20 μ m (**Figure 1**). The corrosion appeared to proceed uniformly, with the corrosion products forming a compact layer limiting the permeation of the corrosive environment to the surface of the AZ31 alloy. The mass loss of AZ31 alloy was 8.3 \pm 0.8 mg/cm² after one week of immersion in AU at 37 °C. This mass loss corresponds to a corrosion rate of 2.5 \pm 0.2 mm/year (density was based on magnesium, 1.74 g/cm³).

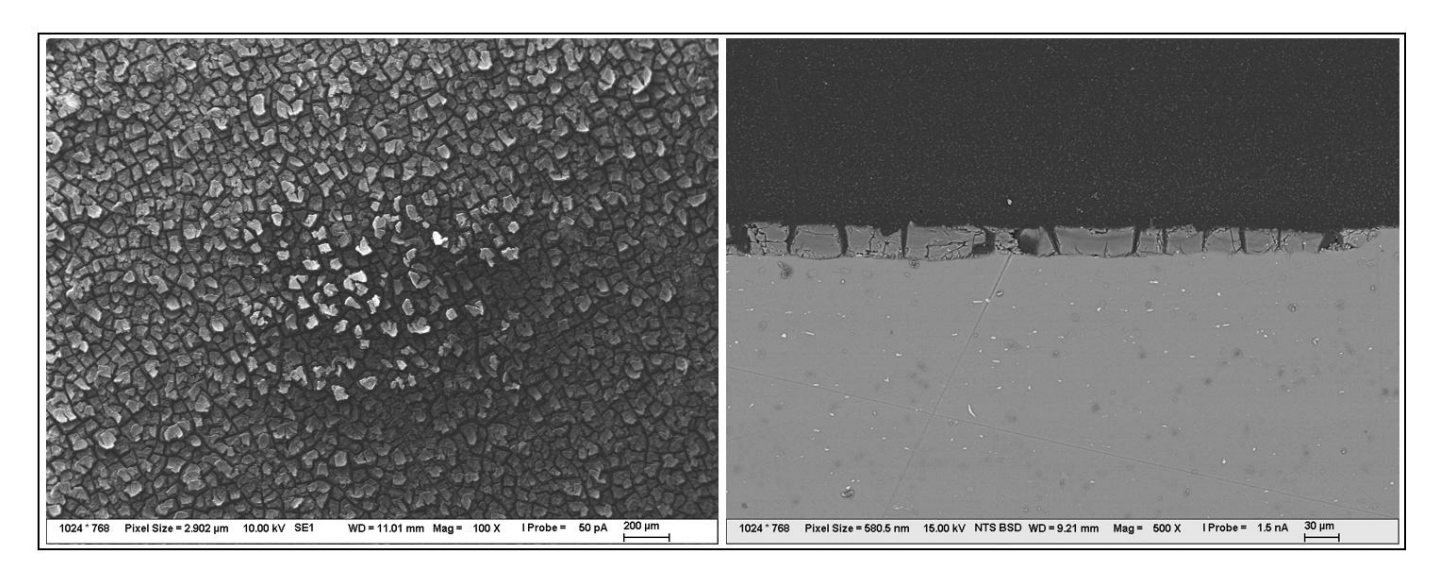


Figure 1 SEM analysis of surface (left) and cross section (right) of AZ31 alloy after 7 days of corrosion in AU

Table 2 EDS analysis of corrosion products on AZ31 alloy after 7 days of corrosion in AU

Element	Weight %	Atomic %
С	7.5	12.4
0	47.4	58.6
Na	1.5	1.3
Mg	11.	9.5
Al	5.6	4.1
Р	20.5	13.1
K	2.1	1.1
Ca	14.6	7.2
Zn	1.9	0.6
N	2.7	3.8

The corrosion products were mainly composed of the elements O, P, Ca, C, Mg and N as shown by EDS analysis (**Table 2**). With respect to FTIR, it is assumed that the corrosion products were mainly composed of



phosphates (e.g. brushite, newberyite and struvite) and minor magnesium carbonate. While the presence of newberyite and struvite is consistent with published work, the absence of brucite is surprising [8]. This discrepancy between our results and the literature can most likely be attributed to differences in the chemical composition of the artificial urine.

PDP measurements for 1 h and 48 h showed (**Figure 2**) that the corrosion properties of AZ31 alloy improved both kinetically and thermodynamically during the AU immersion, as the corrosion current value decreased from $57.8 \,\mu\text{A/cm}^2$ to $32.8 \,\mu\text{A/cm}^2$ and the corrosion potential shifted slightly to more positive values from -1.63 to -1.61 V. The curves also present that after 48 h, the cathodic and anodic reactions were slowed down, indicating that the surface of AZ31 was covered with corrosion products that effectively prevented corrosion.

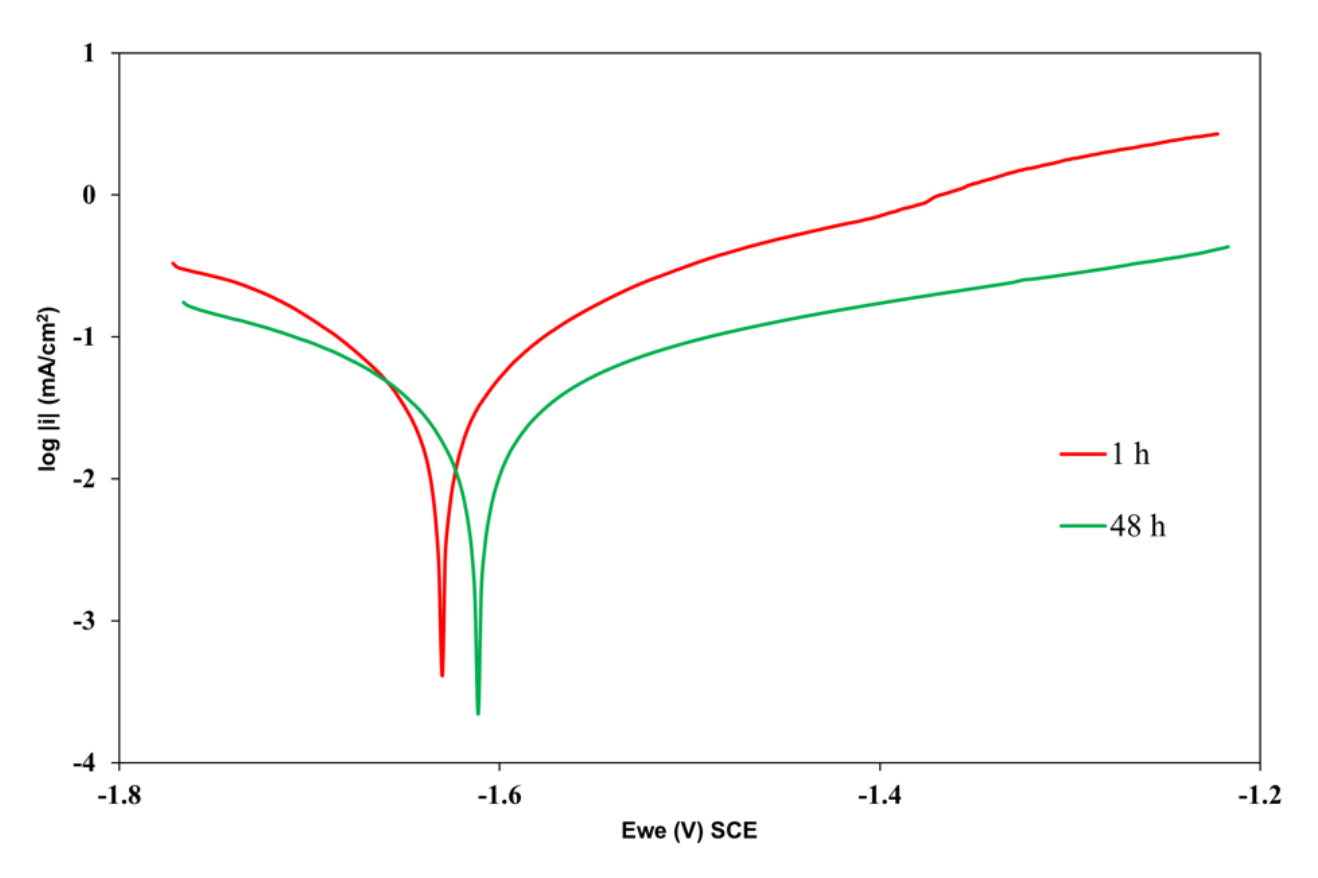


Figure 2 PDP curves for AZ31 alloy in AU after 1 h and after 48 h. The graph expresses the dependence of current density (i) on the potential (E), which is related to the saturated calomel electrode (SCE)

FTIR analysis (**Figure 3**) revealed a dominant band of 1005 cm⁻¹, which was attributed to phosphate [11]. The occurrence of struvite could be related to bands around 1410 cm⁻¹ and 1610 cm⁻¹, which could correspond to NH₄⁺ vibration. However, the bands may also overlap with carbonate and water vibrations. The absence of a band at 3696 cm⁻¹ indicates that Mg(OH)₂ was not formed. To better identify corrosion products, analyses using more advanced methods such as XRD and XPS will be performed in the future.

These preliminary results suggest that AZ31 alloy could be a suitable candidate for the preparation of urological stents. However, for further research it will be necessary to perform corrosion tests also under dynamic conditions, which may differ significantly from static conditions.



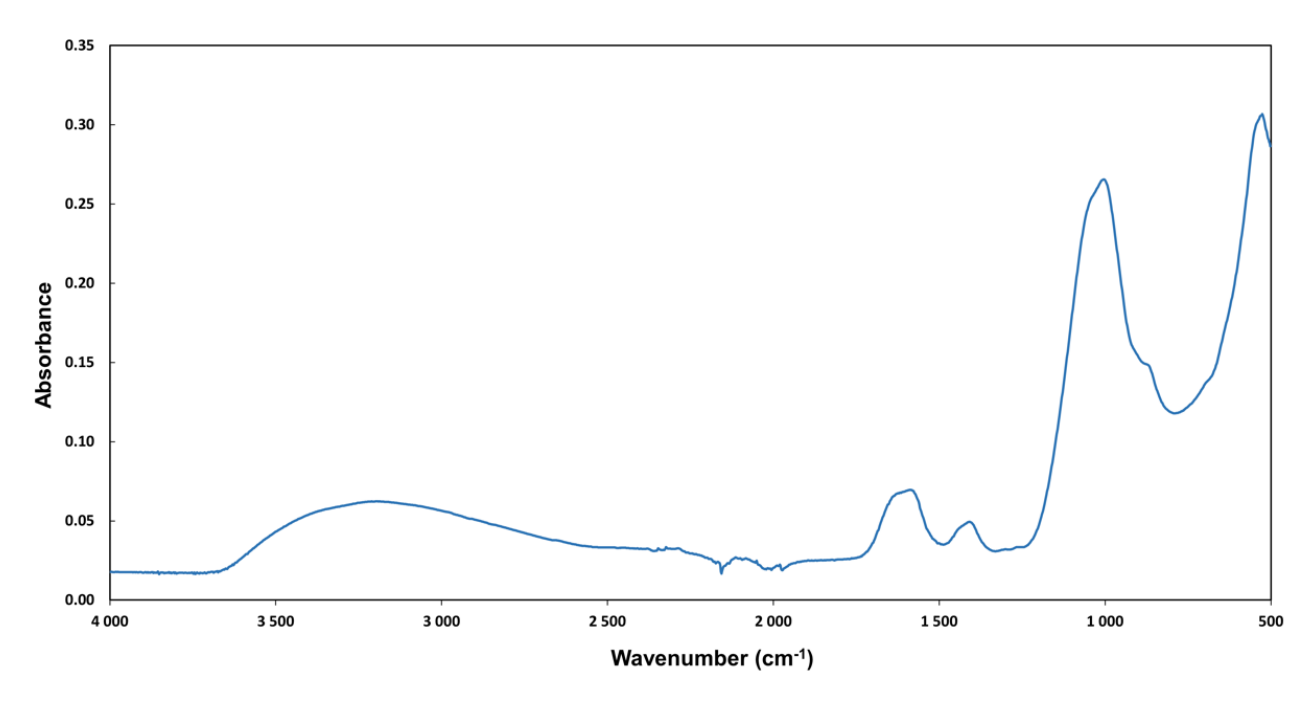


Figure 3 FTIR analysis of corrosion products after 7 days of corrosion of AZ31 in AU

4. CONCLUSION

The corrosion behaviour of AZ31 magnesium alloy was investigated in artificial urine (AU). The first results suggested that AZ31 alloy is a suitable candidate for the study of potential magnesium alloys usable as ureteral stent. The corrosion resistance of AZ31 alloy increased over time, thus there was no uncontrolled degradation of the material. The corrosion products consisted mainly of phosphates such as brushite, newberyite and struvite. The corrosion proceeded uniformly and the thickness of the corrosion products was about 20 µm after one week.

ACKNOWLEDGEMENTS

This work was supported by Specific University Research at FCH BUT, Project Nr. FCH-S-25-8826,
Ministry of Education, Youth and Sports of the Czech Republic.

REFERENCES

- [1] ESMAILY, M., SVENSSON, J.E., FAJARDO, S., BIRBILIS, N., FRANKEL, G.S., VIRTANEN, S., ARRABAL, R., THOMAS, S., JOHANSSON, L.G. Fundamentals and advances in magnesium alloy corrosion. *Progress in Materials Science*. 2017, vol. 89, pp. 92-193. Available from: https://doi.org/10.1016/j.pmatsci.2017.04.011.
- [2] STAIGER, M. P., PIETAK, A. M., HUADMAI, J., DIAS, G. Magnesium and its alloys as orthopedic biomaterials: A review. *Biomaterials*. 2006, vol. 27, no. 9, pp. 1728-1734. Available from: https://doi.org/10.1016/j.biomaterials.2005.10.003.
- [3] PAN, C., LIU, X., HONG, Q., CHEN, J., CHENG, J., ZHANG, Q., MENG, L., DAI, J., YANG, Z., WANG, L. Recent advances in surface endothelialization of the magnesium alloy stent materials, *Journal of Magnesium and Alloys*. 2023, vol. 11, no. 1, 2023, pp. 48-77. Available from: https://doi.org/10.1016/j.jma.2022.12.017.
- [4] DOSKOČIL, L., ŠOMANOVÁ, P., MÁSILKO, J., BUCHTÍK, M., HASOŇOVÁ, M., KALINA, L., WASSERBAUER, J. Characterization of prepared superhydrophobic surfaces on AZ31 and AZ91 alloys etched with ZnCl₂ and SnCl₂. *Coatings*. 2022, vol. 12. Available from: https://doi:10.3390/coatings12101414.
- [5] BERNASCONI, V., TOZZI, M., PIETROPAOLO, A., DE CONINCK, V., SOMANI, B.K., TAILLY, T., BRES-NIEWADA, E., MYKONIATIS, I., GREGORI, A., TALSO, M. Comprehensive overview of ureteral stents based on



- clinical aspects, material and design. *Central European Journal of Urology*. 2023, vol. 76, no. 1, pp. 49-56. Available from: https://doi:10.5173/ceju.2023.218.
- [6] WEN, K., LI, Z., LIU, J., ZHANG, C., ZHANG, F., LI, F. Recent developments in ureteral stent: Substrate material, coating polymer and technology, therapeutic function. *Colloids and surfaces, B, Biointerfaces.* 2024, vol. 238. Available from: https://doi:10.1016/j.colsurfb.2024.113916.
- [7] MEI, D., WANG, C., NIENABER, M., PACHECO, M., BARROS, A., NEVES, S., REIS, R. L., ZHU, S., BOHLEN, J., LETZIG, D., GUAN, S., ZHELUDKEVICH, M. L., LAMAKA, S. V. Corrosion behavior of Mg wires for ureteral stent in artificial urine solution. *Corrosion science*. 2021, vol. 189. Available from: https://doi:10.1016/j.corsci.2021.109567.
- [8] PACHECO, M., AROSO, I.M., SILVA, J.M., LAMAKA, S.V., BOHLEN, J., NIENABER, M., LETZIG, D., LIMA, E., BARROS, A.A., REIS, R.L. Understanding the corrosion of Mg alloys in in vitro urinary tract conditions: A step forward towards a biodegradable metallic ureteral stent. *Journal of Magnesium and Alloys*. 2023, vol. 11, no. 11, pp. 4301-4324. Available from: https://doi.org/10.1016/j.jma.2023.10.002.
- [9] ZHANG, S., BI, Y., LI, J., WANG, Z., YAN, J., SONG, J., SHENG, H., GUO, H., LI, Y. Biodegradation behavior of magnesium and ZK60 alloy in artificial urine and rat models. *Bioactive Materials*. 2017, vol. 2, no. 2, pp. 53-62. Available from: https://doi:10.1016/j.bioactmat.2017.03.004.
- [10] SARIGUL, N., KORKMAZ, F., KURULTAK, I. A new artificial urine protocol to better imitate human urine. *Scientific Reports*. 2019, vol. 9, no. 1. Available from: https://doi.org/10.1038/s41598-019-56693-4.
- [11] SIDORCZUK, D., KOZANECKI, M., CIVALLERI, B., PERNAL, K., PRYWER, J. Structural and optical properties of struvite. Elucidating structure of infrared spectrum in high frequency range. *The Journal of Physical Chemistry A*. 2020, vol. 124, no. 42, pp. 8668-8678. Available from: https://doi:10.1021/acs.jpca.0c04707.